

Contact position controlling for two-dimensional motion bodies by the boundary element method

Junping Pu and Yuanfeng Wang

School of Civil Engineering and Architecture, Northern Jiaotong University, Beijing 100044, China

(Received 2001-05-14)

Abstract: An algorithm is presented for controlling two-dimensional motion contact bodies with conforming discretization. Since a kind of special boundary element is utilized in the algorithm, the displacement compatibility and traction equilibrium conditions at nodes can be satisfied simultaneously in arbitrary locations of the contact interface. In addition, a method is also proposed in which the contact boundary location can be moved flexibly on the possible contact boundary. This method is effective to deal with moving and rolling contact problems on a possible larger moving or rolling contact region. Numerical examples show effectiveness of the presented scheme.

Key words: boundary element method; contact; move; roll

[This work was financially supported by the National Nature Science Foundation of China (No.19902001), the National Excellent Youth Teacher Foundation of China (RJS2001-39) and NJTU Foundation of China (PD-150).]

Contact problems are often encountered in engineering structures and mechanical designs. Since pressure actions in the contact area, it often induces the components and parts of mechanisms and structures to be destroyed at local, and then causes structural invalidation. Therefore, contact problems receive extensive recognition in engineering practices and designs. With analytical methods to tackle contact problems has a large limitation, it can only solve these kinds of problems which have an ideal geometrical shape with frictionless. In recent years, using numerical methods to solve engineering practical problems in contact has received great development. Among these numerical methods, two kinds of typical methods, namely, the finite element method (FEM) and the boundary element method (BEM), have played an important role in solving contact problems [1-13]. With the BEM we just require plotting meshes in those boundary zones in which we are primarily interested, it can reduce effectively the dimension of the problems. As discretization is only done at boundary, the calculation results are more exact than those with the FEM, especially for boundary condition nonlinear problems as contact cases. For the system of equations, variables are just tractions and displacements, hence we can impress exactly contact constraints on the contact interface, no other variables needs to be introduced into the system

of equations. If friction conditions are considered, then the coulomb friction law and incremental theory have to be used. For every load increment an iterative process has to be performed to find the separation, adhesion and slipping area respectively. For the sake of guarantee of the displacement compatibility and traction equilibrium in the contact interface, early works is to adopt a kind of ideal discretization form (node-to-node) in the contact surface [14,15]. Afterward, a kind of interpolation algorithm, which utilizes the shape function to impress interfacial constraint conditions (node-to-point) so that prevents penetration between the contact surfaces, was developed [16-19]. The latter is more suitable for dealing with the non-conforming in the contact interface, such as elastic bodies and rigid bodies in contact, large deformation as well as moving contact problems *etc.* In this paper, a moving contact scheme, in which the displacement compatibility and traction equilibrium can be satisfied at an arbitrary location, has been utilized [20]. Extending the scheme to rolling contact problems is also effective. To theoretically speaking, no matter how far a body moving or rolling, the system of equations should be solvable.

1 Contact constraint conditions

Two bodies A and B in contact with friction are

considered. The contact constraint conditions, corresponding to Cartesian global coordinate and local coordinate systems, can be written as follows respectively according to the incremental theory.

(1) In the global coordinate systems.

Traction equilibrium conditions in the y direction:

$$\Delta T_y^A + \Delta T_y^B = \mathbf{0} \quad (1)$$

in a sticking region,

$$\Delta T_x^A + \Delta T_x^B = \mathbf{0} \quad (2)$$

and in a slipping region,

$$\Delta T_x^K \pm \mu \Delta T_y^K = \mathbf{0}, \quad K = A, B \quad (3)$$

Displacement compatibility conditions in the y direction:

$$\Delta u_y^A - \Delta u_y^B = \delta_y \quad (4)$$

and in a sticking region,

$$\Delta u_x^A - \Delta u_x^B = \mathbf{0} \quad (5)$$

Necessary conditions in the y direction:

$$\Delta T_y^K \leq \mathbf{0}, \quad K = A, B \quad (6)$$

The conditions for determining friction direction:

$$\Delta t_x^K (\Delta u_x^A - \Delta u_x^B) \leq \mathbf{0}, \quad K = A, B \quad (7)$$

(2) In the local coordinate systems.

Traction equilibrium conditions in the normal direction:

$$\Delta T_n^A - \Delta T_n^B = \mathbf{0} \quad (8)$$

in a sticking region,

$$\Delta T_t^A - \Delta T_t^B = \mathbf{0} \quad (9)$$

and in a slipping region,

$$\Delta T_t^K \pm \mu \Delta T_n^K = \mathbf{0}, \quad K = A, B \quad (10)$$

Displacement compatibility conditions in the normal direction:

$$\Delta u_n^A + \Delta u_n^B = \delta_n \quad (11)$$

and in a sticking region,

$$\Delta u_t^A + \Delta u_t^B = \mathbf{0} \quad (12)$$

Necessary conditions in the normal direction:

$$\Delta T_n^K \leq \mathbf{0}, \quad K = A, B \quad (13)$$

The conditions for determining friction direction:

$$\Delta t_t^K (\Delta u_t^A + \Delta u_t^B) \leq \mathbf{0}, \quad K = A, B \quad (14)$$

2 Contact algorithm in the BEM

The boundary element method is to utilize the

weighted residual methods or Betti mutual work theorem to establish the boundary integral equation of equivalence with differential equations. For elasticity theory problems the BEM is to substitute Kelvin fundamental solution into Betti mutual work theorem to get Somigliana integral identity. For the contact problems the BEM is to assemble two sets of boundary integral equations as a large system of equations:

$$C_{\alpha\beta}^K(p) \Delta u_\beta^K(p) + \int_s t_{\alpha\beta}^{*K}(p, q) \Delta u_\beta^K(q) ds(q) = \int_s u_{\alpha\beta}^{*K}(p, q) \Delta t_\beta^K(q) ds(q), \quad K = A, B \quad (15)$$

where s is the whole borderline, $\Delta u_\beta^K(p)$ denotes the displacement incremental value at the point p along the β direction, $\Delta t_\beta^K(q)$ and $\Delta u_\beta^K(q)$ denote the traction and displacement incremental values at the point q along β direction, respectively, $u_{\alpha\beta}^{*K}(p, q)$ and $t_{\alpha\beta}^{*K}(p, q)$ correlate to the displacement and traction fundamental solutions, respectively. The coefficient items $C_{\alpha\beta}^K(p)$ lie on the geometry shape at the point p and can be evaluated by incorporating with the singular matrix items at main diagonal by means of the rigid body displacement method. With the boundary constraint conditions of formulas (1)-(7) or (8)-(14), the displacement and traction components can be solved in the whole borderline.

By discretization and interpolation for the boundary integral equation (15), a set of matrix equations can be written as

$$H^K \Delta u^K = G^K \Delta t^K, \quad K = A, B \quad (16)$$

Hence, matrix equation (16) with the boundary constraint conditions (1)-(7) or (8)-(14) buildup a set of whole numerical algorithm formulations of contact problems. Since the traction cannot be accurately described using a quadratic interpolation function in a contact zone, a kind of linear element is developed in the paper, this kind of element is simply and flexible for dealing with moving contact problems.

3 Boundary stresses

Since boundary stresses cannot be immediately solved according as the boundary integral equation, a feasible way is to utilize numerical integral to get tractions and displacements at the boundary, and then utilize geometry equations and generalized Hooke law to determine boundary stresses approximatively. For planar strain problems the equations can be listed as follows:

$$\sigma_{\alpha\beta} n_\beta = \frac{2G\nu}{1-2\nu} n_\alpha u_{\beta,\beta} + G n_\beta (u_{\alpha,\beta} + u_{\beta,\alpha}) = t_\alpha \quad (17)$$

$$\frac{\partial u_\alpha}{\partial x_\beta} \frac{\partial x_\beta}{\partial \xi} = \frac{\partial u_\alpha}{\partial \xi} \quad (18)$$

In the set of linear algebra equations (17) and (18) there are 4 unknown quantities $u_{\alpha,\beta}$. After getting hold of $u_{\alpha,\beta}$ with the numerical method, these results are substituted into a formula with regard to the stress and strain, and then the stress components $\sigma_{\alpha\beta}$ at an arbitrary point in the boundary can be solved. With coordinate transformation the unknown stress components σ_i along the borderline can be solved according to the state of stress at one point. In Cartesian coordinate systems the coordinate, displacement and their variety ratio can be written as

$$\mathbf{x} = \begin{Bmatrix} x_1 \\ x_2 \end{Bmatrix} = \begin{bmatrix} N_1 & 0 & N_2 & 0 \\ 0 & N_1 & 0 & N_2 \end{bmatrix} \begin{Bmatrix} x_{11} \\ x_{12} \\ x_{21} \\ x_{22} \end{Bmatrix} = \mathbf{N}\mathbf{x}^e \quad (19)$$

$$\mathbf{u} = \begin{Bmatrix} u_1 \\ u_2 \end{Bmatrix} = \begin{bmatrix} N_1 & 0 & N_2 & 0 \\ 0 & N_1 & 0 & N_2 \end{bmatrix} \begin{Bmatrix} u_{11} \\ u_{12} \\ u_{21} \\ u_{22} \end{Bmatrix} = \mathbf{N}\mathbf{u}^e \quad (20)$$

where,

$$N_1 = \frac{1}{2}(1 - \xi), \quad N_2 = \frac{1}{2}(1 + \xi) \quad (21)$$

the first derivative of x_1 , x_2 , u_1 and u_2 with respect to ξ are, respectively

$$\frac{\partial x_1}{\partial \xi} = \frac{1}{2}(x_{12} - x_{11}), \quad \frac{\partial x_2}{\partial \xi} = \frac{1}{2}(x_{22} - x_{21}) \quad (22)$$

$$\frac{\partial u_1}{\partial \xi} = \frac{1}{2}(u_{12} - u_{11}), \quad \frac{\partial u_2}{\partial \xi} = \frac{1}{2}(u_{22} - u_{21}) \quad (23)$$

substituting these derivative values into formula (24), the stress components can be numerically solved as

$$\sigma_{\alpha\beta} = 2G \frac{\nu}{(1-2\nu)} \delta_{\alpha\beta} \frac{\partial u_k}{\partial x_k} + G \left(\frac{\partial u_\alpha}{\partial x_\beta} + \frac{\partial u_\beta}{\partial x_\alpha} \right) \quad (24)$$

$\alpha, \beta, k = 1, 2$

4 Method for moving and rolling contact problems

On a possible contact zone, elements are tackled as a kind of special boundary linear elements. These elements consist of two fixed nodes at the ends, and the middle node of each element can be tackled as a moveable node following the element changing (white point). When contact taking place, the fixed node (black point) on the surface of a body contact with the

arbitrary point (white point) on the surface of another body, and then this movable white point can divide the element again and overlap with the fixed black point, see **figure 1**.

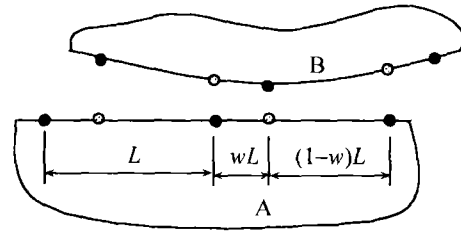


Figure 1 Body B moving relatively to body A. Black point — fixed node, and white point — moveable node.

Contact elements and separate elements are considered as two sub-elements in possible contact regions (from block end nodes to white middle nodes), the contact state should be checked for each sub-element. The distributing of tractions and displacements are supposed as subsection linear interpolation functions in these kind of special elements: there are the linear distributing between the end nodes and movable nodes. The displacement is continuous at each node, but the traction can be discontinuous at each node. As a non-linear problem, an increment algorithm is needed to solve the system of equations. For each increment step, the movable nodes of contact elements are on different locations. **Figure 2** shows the interpolation function for the increment from step N to $N + 1$. The possible discontinuity of tractions is accomplished by the definition of t^- and t^+ , two different variables at each boundary node. With iteration the actual contact regions will be made certain gradually. Using this method, among the coefficient items that consist of the sum of integration of the kernel functions multiplied by the shape functions in the corresponding elements, those items to be modified to make up only a very small portion in the total coefficient matrix equations. And most of the influence coefficients are all keep fixedness. For this contact manner of nodes to movable points, the element variable mode can be expressed as

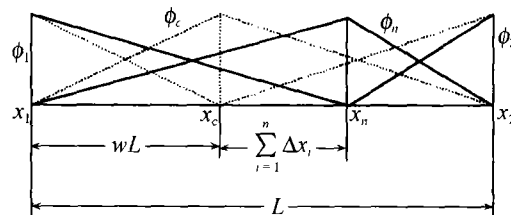


Figure 2 Element variable mode and interpolation function.

$$\phi^{(e)}(x) = N_1 \phi_1 + N_n \phi_n =$$

$$\frac{\phi_1}{2} \left(1 - \frac{2(x - x_1) - wL - \sum_{i=1}^n \Delta x_i}{wL + \sum_{i=1}^n \Delta x_i} \right) + \frac{\phi_n}{2} \left(1 + \frac{2(x - x_1) - wL - \sum_{i=1}^n \Delta x_i}{wL + \sum_{i=1}^n \Delta x_i} \right) \quad (25)$$

where, x is a location coordinate for an arbitrary point in the element, x_i are the node coordinates, N_i are the interpolation functions, ϕ_i are variables including displacements and tractions, L is the element length, w is a factor of proportionality.

While the factor of proportionality $w > 0$, the fixed end nodes (black point) on the surface will take place a dislocation and contact with the opposite movable points (white point) on the other surface in the contact interfaces. However, $w = 0$ means a traditional node-pairs form, $w = 0.5$ means the movable point to be in the middle location between the two end nodes, this case corresponding to the primary element density of the contact node-pairs form is increased by one time. By virtue of this scheme, together organically the advantage of the contact node-pairs with the agility of the interpolation function mentioned above, both the equilibrium relations of tractions and the compatibility of displacements for the corresponding nodes of a contact zone can all be guaranteed.

For the moving contact problem, if body B moves forward but body A is fixed, then the black points on body A keep fixedness, the black point of body B move forward. On the contact interfaces of bodies A and B, there have white points corresponding to the moving and immovable black points, respectively. In this way, the displacement compatibility and the traction equilibrium condition can be satisfied while body B slides over body A at an arbitrary location.

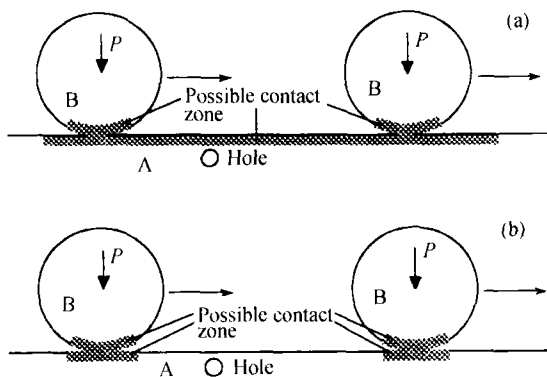


Figure 3 Moving contact scheme.

While a body moving forward, the whole slipping contact zone must be served prior as the possible contact zone, shown as **figure 3(a)**. Since the freedom degree is 4 for each node in a possible contact zone, it is one times more than the freedom degree of the impossible contact zone. Thus the farther the distance of body B moving, the larger the size for evaluating a coupled set of linear algebra equations. If the moving distance of body B exceeds a definite scope, then the solving will not be performed. To solve this problem, we develop a kind of solving scheme, in which the possible contact boundary location can be moved flexibly at the whole possible contact boundary, shown as figure 3(b). Since the possible contact zone is plotted prior too big so that the size of the set of algebra equations will be huge and then the system of equations would not be solved while body B moves in a big scale range, the problem could be solved. By using this method, the problem can be solved while body B moves to an arbitrary far distance, but the size of the system of equations is same as static contact problems, so the computing time could be reduced greatly. While body B is in moving, the location of a contact point can be denoted as

$$x = x_0 + \frac{l}{2} \{ [1 + (-1)^k] \text{int}(kw) + [1 + (-1)^{k-1}] \times \text{int}[(k-1)w] \} + l[k \cdot w - \text{int}(kw)], \quad k = 1, 2, \dots, N_{\text{step}} \quad (26)$$

where, x_0 is a original location, w is a proportional factor of the moving distance (see figure 1), and content to the condition $0 \leq w \leq 1$.

For the rolling contact problem, the whole wheel edge and the surface on which the wheel will come by are all possible contact zones, shown as **figure 4(a)**. The farther the distance of the wheel rolling, the larger the size of the coupled set of linear algebra equations, also we can use the upper method to treat with this problem. After the wheel was rolled some distance

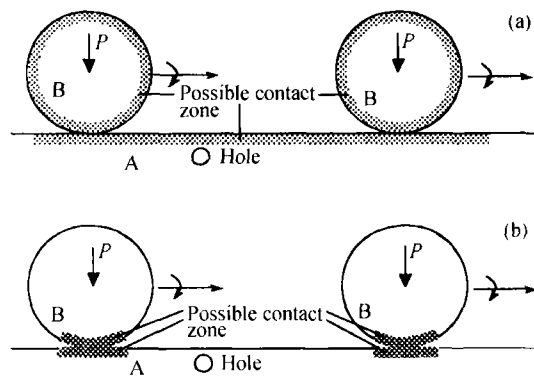


Figure 4 Rolling contact scheme.

forward, the possible contact zone on body A was moved forward a corresponding distance along with the wheel rolling. The possible contact zone of the edge of wheel B would be switched back counter-clockwise a corresponding arc length, and the arc length is equal to the rolling distance, see figure 4(b). In this way, no matter how far the wheel was rolled forward, the size of the possible contact zone, which had to be determined in advance, is equal to the size of the static contact case. In the wheel center, after the wheel was rolled forward an element length, the zone on which the load was applied would be turned counter-clockwise a corresponding angle, hence the direction of load acting was always vertical downwards at each location.

While wheel B is in rolling, the locations of various points can be described as follows (see figure 5), respectively. Hereinto, the locations of the reference points 1 and 3 can be written as

$$\begin{aligned}
 x_{1,3}^K &= x_0 + R \sum_{i=1}^K \Delta\varphi_i + OC \cdot \sin\left(\varphi_0 - \sum_{i=1}^K \Delta\varphi_i\right) \pm \\
 &r \cos\left(\varphi_0 - \sum_{i=1}^K \Delta\varphi_i\right), \\
 y_{1,3}^K &= H_A + R - \\
 &\left[OC \cdot \cos\left(\varphi_0 - \sum_{i=1}^K \Delta\varphi_i\right) \mp r \sin\left(\varphi_0 - \sum_{i=1}^K \Delta\varphi_i\right) \right], \\
 K &= 1, 2, \dots, n
 \end{aligned} \tag{27}$$

and that the locations of the reference points 2 and 4 will be denoted as

$$\begin{aligned}
 x_{2,4}^K &= x_0 + R \sum_{i=1}^K \Delta\varphi_i + (OC \pm r) \sin\left(\varphi_0 - \sum_{i=1}^K \Delta\varphi_i\right), \\
 y_{2,4}^K &= H_A + R - (OC \pm r) \cos\left(\varphi_0 - \sum_{i=1}^K \Delta\varphi_i\right), \\
 K &= 1, 2, \dots, n
 \end{aligned} \tag{28}$$

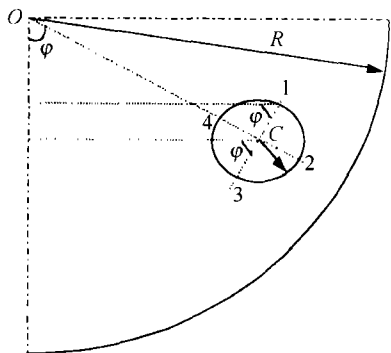


Figure 5 Determining of the location of various points.

where, $\Delta\varphi_i$ is a rotational increment of wheel B while the wheel is in rolling, R is a radii of wheel B, r

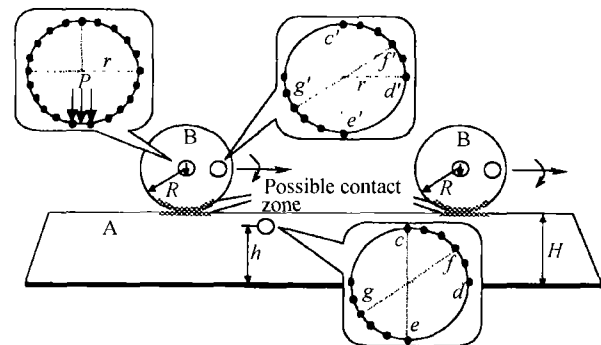
is a radii of a small hole on the wheel, φ_0 is a original angle with respect to the original location, H_A is a plane altitude of contact body A, and n is the node number on the edge of the hole in the wheel. If $OC = R$ and $r = 0$, the above-mentioned formulas will be reduced into the coordinates of the point of edge on the wheel as follows:

$$\begin{aligned}
 x^K &= x_0 + R \sum_{i=1}^K \Delta\varphi_i + R \sin\left(\varphi_0 - \sum_{i=1}^K \Delta\varphi_i\right), \\
 y^K &= H_A + R \left(1 - \cos\left(\varphi_0 - \sum_{i=1}^K \Delta\varphi_i\right)\right), K = 1, 2, \dots, m
 \end{aligned} \tag{29}$$

where, m is the node number on the edge of the wheel.

5 Numerical examples

Wheel B rolls on an elastic foundation at a uniform speed at a horizontal distance of 15.912 mm from the hole center of body A. There is a circular hole inside body A near the contact interface, the radii $r = 0.125$ mm, and the vertical distance from the hole center to ground is 39 mm. Along the hole edge there are 20 linear elements, and on body A there are 120 linear elements. However, on body B there is a circular hole near the wheel edge, the distance from the hole center to the wheel center is 9 mm, the radii r of hole is 0.125 mm, and the external load P is applied over the 21 linear elements in the center of the wheel. There are merely 24 linear elements on the possible contact zone, 145 linear elements are divided on wheel B, and the rest parameters refer to figure 6. Now let us seeing about the stresses changing of nodes on the edge of both hole bodies A and B while wheel B rolls on the surface of elastic foundation A.



$P = 5 \text{ N/mm}$, $R = 10 \text{ mm}$, $r = 0.125 \text{ mm}$, $H = 40 \text{ mm}$
 $h = 39 \text{ mm}$, $\nu_A = \nu_B = 0.3$, $E_A = E_B = 4 \text{ kN/mm}^2$
 Hertz: $\sigma_{\max} = 18.69 \text{ N/mm}^2$

Figure 6 Wheel B with a circular hole rolls on the surface of body A with a circular hole.

By calculation it is known that on the point c of the

edge of hole along the tangent direction, there are the maximum tensile stresses, but on the point d of the edge of hole along the tangent direction there are the maximum compress stresses on foundation A. After

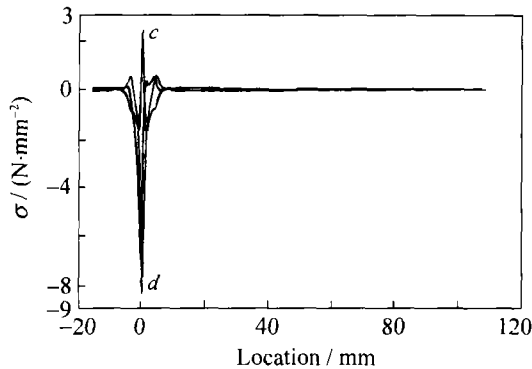


Figure 7 Stress changing of the hole edge on foundation A after two circle rolling of wheel B.

6 Conclusions

A kind of method, which can flexibly transform contact element length, has been given. A unable overcoming difficulty using the conventional node-pairs contact method, in which the displacement compatibility and the traction equilibrium conditions cannot be satisfied while contact bodies moving, is solved. The method provides a means for moving contact problems while nodes dislocate continuously from a node to another in the contact zone.

Another kind of method in which the contact boundary location can be moved flexibly at a possible contact zone is also put forward. By means of the algorithm, the problem, since the possible contact zone has to be setup more larger in advance so that the size of the coupled set of algebra equations is huge and that has a difficulty for solution of moving problems at a great scale range, is solved. Extending this thoughtway to the rolling contact problems, a difficult problem, of which the whole wheel edge will be regard as the possible contact boundary so that the freedom degree of the system of equations is too big, is also solved.

References

- [1] S.K. Chan and I.S. Tuba, A finite element method for contact problems of solid bodies-part I. Theory and validation [J], *Int.J. Mech.Sci.*, 13(1971), p.615.
- [2] S.K. Chan and I.S. Tuba, A finite element method for contact problem of solid bodies-part II. Application to turbine blade fastenings [J], *Int. J. Mech. Sci.*, 13(1971), p.627.
- [3] E.A. Wilson and B. Parson, Finite element analysis of elastic contact problems using differential displacements

two-circles rolling of wheel B on elastic foundation A, the stress changes of hole edge nodes along the tangent direction for elastic foundation A and wheel B are shown as figures 7 and 8, respectively.

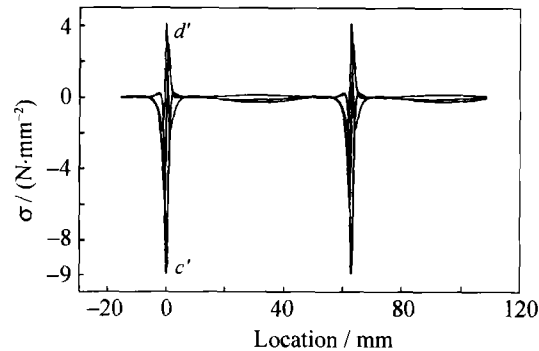


Figure 8 Stress changing of the hole edge on wheel B after two circle rolling of wheel B.

- [J], *Int. J. Numer. Meth. Engng.*, 2(1970), p.387.
- [4] A. Francavilla and O.C. Zienkiewicz, A note on numerical computation of elastic contact problems [J], *Int. J. Numer. Meth. Engng.*, 9(1975), p.913.
- [5] B. Fredriksson, Finite element solution of surface nonlinearities in structural mechanics with special emphasis to contact and fracture mechanics problems [J], *Comput. Struct.*, 6(1976), p.281.
- [6] N. Okamoto and M. Nakazawa, Finite element incremental contact analysis with various frictional conditions [J], *Int. J. Numer. Meth. Engng.*, 14(1979), p.337.
- [7] K. J. Bathe and A. Chaudhary, A solution method for planar and axisymmetric contact problems [J], *Int. J. Numer. Meth. Engng.*, 21(1985), p.65.
- [8] Y. Ezawa and N. Okamoto, Development of contact stress analysis programs using the hybrid method of FEM and BEM [J], *Comput. Struct.*, 57(1995), No.4, p.691.
- [9] A. Landenberger and A. El-Zafrany, Boundary element analysis of elastic contact problems using gap finite elements [J], *Comput. Struct.*, 71(1999), No.6, p.651.
- [10] K. Yamazaki, J. Sakamoto, and S. Takumi, Penalty method for three-dimensional elastic contact problems by boundary element method [J], *Comput. Struct.*, 52(1994), No.5, p.895.
- [11] S. Simunovic and S. Saigal, Quadratic programming contact formulation for elastic bodies using boundary element method [J], *AIAA J.*, 33(1995), No.2, p.325.
- [12] J. G. Leahy and A. A. Becker, The numerical treatment of local variables in three-dimensional frictional contact problems using the boundary element method [J], *Comput. Struct.*, 71(1999), No.4, p.383.
- [13] R.S. Hack and A.A. Becker, Frictional contact analysis under tangential loading using a local axes boundary element formulation [J], *Int. J. Mech. Sci.*, 41(1999), p.419.
- [14] T. Andersson, B. Fredriksson, and B.G. Allan-Persson, The boundary element method applied to two-dimensional contact problems, [in] C.A. Brebbia, ed., *New Developments in Boundary Element Methods* [M], CML Publications, 1980, p.247-263.

- [15] M.J. Abdul-Mihsein, A.A. Bakr, and A.P. Parker, A boundary integral equation method for axisymmetric elastic contact problems [J], *Comput. Struct.*, 23(1986), No.6, p.787.
- [16] O.A. Olukoko, A.A. Becker, and R.T. Fenner, A new boundary element approach for contact problems with friction [J], *Int. J. Numer. Meth. Engng*, 36(1993), p.2625.
- [17] F. Paris, A. Blazquez, and J. Canas, Contact problems with nonconforming discretization using boundary element method [J], *Comput. Struct.*, 57(1995), No.5, p.829.
- [18] A. Blazquez, F. Paris, and J. Canas, Interpretation of the problems found in applying contact conditions in node-to-point schemes with boundary element non-conforming discretizations [J], *Int. J. Engng. Anal. Boundary Elements*, 21(1998), p.361.
- [19] A. Lorenzana and J.A. Garrido, A boundary element approach for contact problems involving large displacements [J], *Comput. Struct.*, 68(1998), No.4, p.315.
- [20] Z.H. Yao, J.Q. Chen, and J.P. Pu, Some application and new schemes of two-dimensional BEM for contact problem, [in] L. Gaul and C.A. Brebbia, eds., *Computational Methods in Contact Mechanics IV* [M], WIT Press, 1999, p.251-260.